ARTICLE

JOURNAL OF **Applied Polymer** SCIENCE WILEY

Surface modification of ZnO quantum dots coated polylactic acid knitted fabric for photocatalytic application

Rivaldo Leonn Bezerra Cabral[1] | Felipe Mendonça Fontes Galvão[1] |
Kesia Karina Oliveira de Souto Silva[1] | Brenno Henrique Silva Felipe[2] |
Nivaldo Freire de Andrade Neto[3] | Pierre Basílio de Almeida Fechine[4] |
Andrea Zille[5] | Suyeon Kim[6] | José Heriberto Oliveira do Nascimento[1,2]

[1]Postgraduate Program in Textile Engineering, Center of Technology, Federal University of Rio Grande do Norte, Rio Grande do Norte, Brazil

[2]Postgraduate Program in Mechanical Engineering, Center of Technology, Federal University of Rio Grande do Norte, Rio Grande do Norte, Brazil

[3]Department of Materials Engineering, Center of Technology, Federal University of Rio Grande Do Norte, Rio Grande do Norte, Brazil

[4]Department of Analytical Chemistry and Physical Chemistry, Science Center, Federal University of Ceará, Ceará, Brazil

[5]Center for Textile Science and Technology (2C2T), University of Minho, Guimarães, Portugal

[6]Department of Engineering, Pontificia Universidad Católica del Perú, Lima, Peru

Correspondence
Rivaldo Leonn Bezerra Cabral and José Heriberto Oliveira do Nascimento, Postgraduate Program in Textile Engineering, Center of Technology, Federal University of Rio Grande do Norte, 59072970, Rio Grande do Norte, Brazil.
Email: systemriva38@gmail.com and joseheriberto@ct.ufrn.br

Abstract

In this work, ZnO quantum dots (ZnOQD) were synthesized by Sol–gel synthesis and impregnated on polylactic acid (PLA) knitted fabric through self-assembly of different cycles from layer-by-layer (LBL) using cationic agent Poly(diallydimethylammonium chloride) (PDDA). Then, morphological, chemical and photocatalytic properties were studied. The results demonstrate that the synthesis provided 8 nm Wurtzite-type ZnO nanoparticles. In addition, X-ray photoelectron spectroscopy (XPS) spectra, X-ray diffraction (XRD) and scanning electron microscopy (SEM) proved the inclusion of ZnOQD on the surface of PLA matrix, which allowed the evaluation of its photocatalytic properties, therefore, coated PLA with five cycles of ZnOQD obtained the best result for degrading 85% of the dye Rhodamine B (RhB) in 360 min under UV radiation, in addition to its reusability for another five cycles of photocatalytic activity.

KEYWORDS
layer-by-layer, nanoparticles, photocatalytic, polylactic acid, quantum dots, ZnO

1 | INTRODUCTION

In the last few years, the use of dyes in the textile and leather industry has declined, but even so their production remains large due to the applications of the world of fashion, interior design and plastics. It is estimated that more than 800,000 tons, representing 3000 types of dyes, are produced annually for applications in textile processes, and the lack of efficiency and optimization of these production processes causes the release of about 10%–15% of these dyes in the environment as generators of complex textile effluents.[1,2] As a result, up to 84,000 tons of dyes can be lost in water, 90 million cubic meters of water are used annually in the production of these dyes as well as in their application in the textile and leather industries. These processes end up being

responsible for the production of 20% of the industrial effluents that pollute the waters.[3,4] To reduce water pollution with dyes, several treatments are proposed such as flocculation,[5] adsorption,[6] photocatalysis,[7] among others.

Photocatalysis has been used as an excellent technology to eliminate numerous organic pollutants from different wastewater and convert them into non-toxic substances. This technology mainly uses semiconductor metal oxides as photocatalysts. These oxides have the purpose of degrading organic molecules, such as dyes.[8] The photocatalysis in the presence of semiconductor materials involves a reaction with free radicals initiated by radiation. It is a process in which the semiconductor irradiation produces photoexcited electrons and positively charged gaps. The photoexcitation of semiconductor particles by light with energy greater than the energy gap of the semiconductor, generates an excess of electrons in the conduction band and electronic vacancies (gaps) in the valence band.[9]

There are countless semiconductor catalysts that can be applied to dye photodegradation, such as zinc oxide nanoparticles considered as an excellent photocatalyst in the textile wastewater.[10] Studies has shown that the photocatalytic efficiency of these nanoparticles substantial increase in the photocatalytic activity of ZnO.[11] Mohamed et al. investigate solar photocatalytic performance of ZnOQD in the degradation of synthetic dyes Dianix, methyl orange and comassie brilliant blue R in textile effluents.[12–14] In a later work, this same group evaluated the behavior of ZnOQD to photodegrade the carmine indigo dye and the real effluent from an Egyptian textile industry.[15] Similarly, Khan and researchers reported the photodegradation of methyl orange dye using ZnOQD under UV irradiation.[16] Chen obtained excellent results in the study of ZnO nanoparticles for photocatalytic degradation of Azo dyes under UV irradiation.[17]

ZnO are type II-IV crystalline semiconductors that have recently attracted great attention due to their piezoelectric properties.[13] These nanomaterials can be applied to transistors, biosensors, LED's, photovoltaic cells, antibacterial agents, and heterogeneous photocatalysis processes.[18–23] The characteristics such as structural defects, crystallite size and morphology are due to ZnO having an energy gap of approximately 3.37 eV and a high energy binding of excitons (60 meV).[24] Furthermore, the ZnOQD have the three dimensions of its nanostructure defined on a scale of length between 1 and 10 nm, which provide quantum confinement responsible for increasing its gap and, thus, creating a sufficient distance for the coulombic attraction of transporters load is minimally null.[25] This is an essential characteristic for the excitonic effects to become more expressive and fundamental in the ultraviolet radiation protection on textile fabric and photocatalytic property.[26,27] This property is the result of electron migration to the material surface through the focus of UV radiation and holes that react with the oxygen in the medium, generating active sites forming superoxides capable of degrading organic molecules dye from wastewater, such as found in food and textile industrial effluents.

Recent research has been carried out to evaluate the photocatalytic activity of ZnOQD synthesized by the solvothermal method with size between 8.4 and 9.6 nm. In this work, the researchers verified the sample of smaller size and synthesized at low temperature showed better photocatalytic result, degrading the Dianix Blue dye at a rate of $2.47 \times 10^{-2} \text{ s}^{-1}$.[13] Wang presented that 96.7% of RhB was degraded at the irradiation time of 150 min in the presence of ZnOQD.[28] However, this mechanism is limited thanks to the rapid recombination of the ZnO hole and electron pairs. In addition, ZnOQD powders suspended in the organic dye degradation mechanism in aqueous media may pose a potential risk to the ecosystem due to the complexity of nanostructure retention.[29] In addition, its use in powder form would become an obstacle in the reuse of inorganic semiconductor. One way to get around these obstacles is to implement polymeric matrices such as plastics and textiles. In addition to the retention of nanostructures and the possibility of reuse in photocatalytic cycles, the polymeric material, due to its flexibility, can facilitate the inhibition of electron recombination in the ZnO holes necessary for photodegradation.[30]

In this work, a new material based on ZnOQD coated PLA fibers was produced, thus obtaining a nanocomposite with photocatalytic properties. The colloidal ZnOQD solution was obtained by Sol–gel reaction and immobilized on PLA knitted fabric by LBL self-assembly with cationic polyelectrolyte. Morphological and optical analyzes of ZnOQD were performed, as well as the PLA/ZnOQD nanocomposite were evaluated for its photocatalytic property on RhB dye under UV radiation.

2 | EXPERIMENTAL

2.1 | Materials and chemicals

PLA knitted fabric made in jersey-like structure, 182 g m^{-2} in grammage, average fiber diameter of 11.4 μm and 30 Ne. Zinc acetate dihydrate (Zn [$CH_3COO]_2.2H_2O$), potassium hydroxide (KOH) (99%), ethanol (99.5%) were purchased from Isofar Chemical Industry and used without further purification. RhB dye (CAS number: 81-88-9) A.R. was purchased from Labsynth (100%), to use in the photocatalytic evaluation. The PDDA (300,000 g/mol; 20% wt in H_2O) was purchased from Sigma Aldrich.

SCHEME 1 Flowchart of the layer-by-layer assembly coating [Color figure can be viewed at wileyonlinelibrary.com]
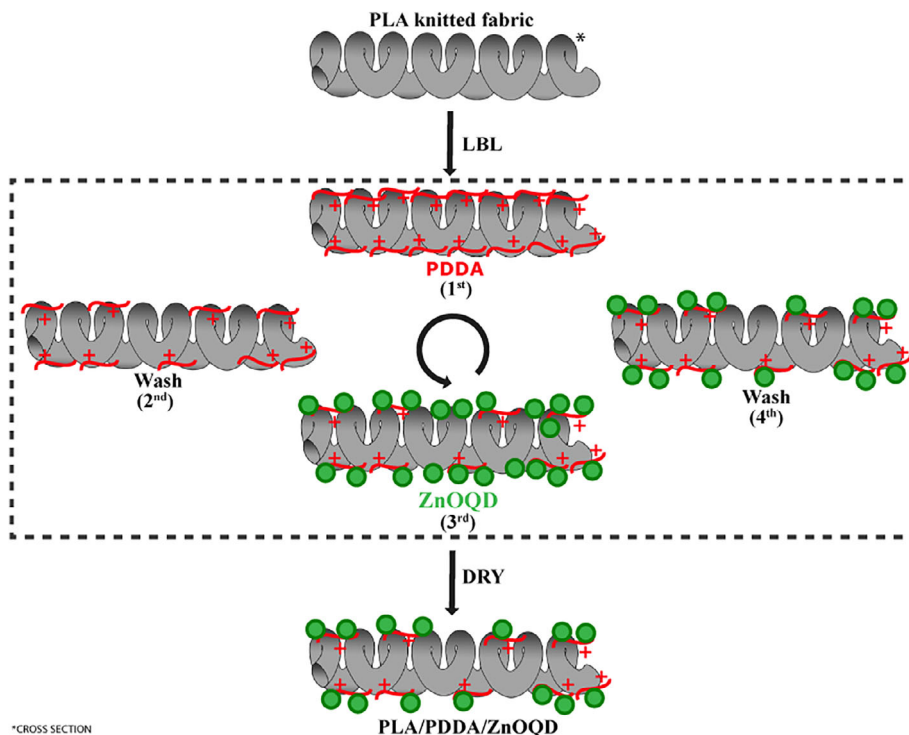
2.2 | Synthesis and purification of ZnOQD

The ZnOQD was obtained by method proposed by Pacholski,[31] however, with some changes. 3.78 g of (Zn [CH$_3$COO]$_2$.2H$_2$O) were diluted in 162 ml of ethanol, under vigorous stirring at 60°C, while 1.86 g of KOH were solubilized in 88 ml of ethanol and ultrasonicated for 5 min at room temperature.

Then, the KOH solution was added dropwise to the precursor solution of Zn(CH$_3$COO)$_2$.2H$_2$O, so that the mixture is stirred vigorously at 60°C for 135 min, then placed at rest until it reaches the temperature of 30°C. At the end of this step, the resulting ZnOQD solution was purified. First, this colloidal solution was washed with ethanol in centrifugation at 4000 rpm for 20 min to separate the quantum dots from the by-products of the ZnOQD synthesis step. The decanted material is put to dry in an oven at 70°C for 30 min, then a fine white powder of ZnOQD is formed.

2.3 | LBL assembly coating

The procedure for making the ZnOQD coated PLA fabric was performed using an automated LBL machine and shown Scheme 1. The PLA fabric samples were cut to 6 x 6 cm measurements, previously washed as described in section 2.1. Afterwards, they were immersed cyclically in an aqueous solution of PDDA at 5 g L^{-1} with pH = 4

(cationic charge) and also, in the ZnOQD solution at 0.8 g L^{-1} with pH = 11 (anionic charge). The immersion time in each cycle was 5 min.

With each immersion of the PLA in cationic and anionic solutions, the samples were immersed in deionized water for 2 min and, at the end of the cycles, the PLA knitted coated were dried in an oven with air circulation at a temperature of 70°C for 35 min. The samples under study in this work are named according to the number of LBL cycles submitted. Thus, the samples in ZN1, ZN3, ZN5, ZN7 and ZN9 were produced from 1, 3, 5, 7 and 9 coating cycles, respectively.

2.4 | Characterization

The structural properties of the ZnOQD, as well as their presence in the PLA fibers, were analyzed by X-ray diffraction (XRD). The apparatus used in the analysis was a Bruker D2 Phaser diffractometer, scanning speed 0.02 deg min^{-1} and using a CuKa source, lattice parameters of ZnOQD has been determined by Equation (1), (2), (3) and (4)[31,32]:

$$d_{hkl} = \frac{1}{\sqrt{\frac{4(h^2+k^2+hk)}{3a^2} + \frac{l^2}{c^2}}} \tag{1}$$

$$a = \frac{\lambda}{\sqrt{3}\, sen\theta_{100}} \tag{2}$$
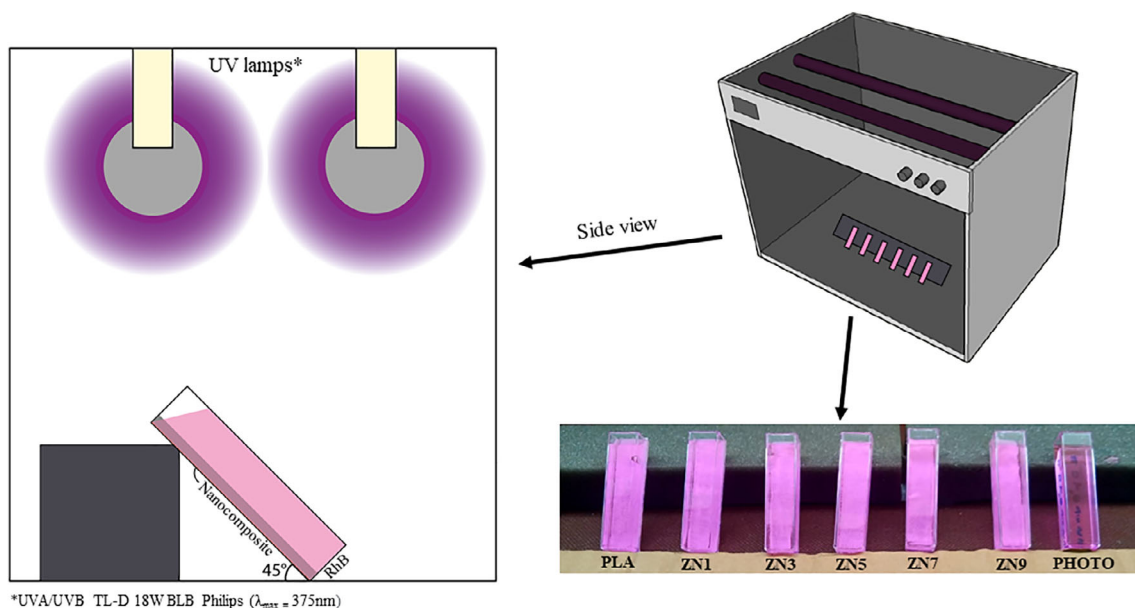
SCHEME 2 Photocatalytic assay scheme of coated samples with and without ZnOQD [Color figure can be viewed at wileyonlinelibrary.com]

$$c = \frac{\lambda}{sen\theta_{002}} \quad (3)$$

$$V = \sqrt{3a^2}\left(\frac{c}{2}\right) \quad (4)$$

where d_{hkl} is interplanar distance in the structure of hexagonal; h, k and l are Miller index; a and c are cell parameters; $\lambda = 1.54$ is wavelength of the x-ray radiation (Cu-Kα radiation); θ_{100} and θ_{002} are Bragg's angle at (100) and (002), respectively, and V is the volume cell for the hexagonal structure. The X-ray photoelectron spectroscopy (XPS) measurement was made in an ultrahigh vacuum VG Scientific ESCALAB 200A spectrometer using a 15 kV (300 W) monochromatic AlKα X-ray. All binding energy (BE) values reported in the present work are with the reference to carbon C1s core level at 284.6 eV. The curve fitting of the high-resolution spectra was performed with combined Gaussian–Lorentzian functions. Transmission electron microscopy (TEM), high-resolution transmission electron microscopy (HRTEM) and selected area electron diffraction (SAED) images were performed with the JEM-2100 JEOL microscope operating at 200 kV and having a resolution of 0.2 nm used to structural properties of ZnOQD. A drop of this solution was deposited on the copper grid covered with a carbon film and placed in the sample holder. Morphological properties of nanocomposites were characterized by Field Emission Scanning Electron Microscopy/Energy dispersive x-ray spectroscopy (FESEM/EDS) analyses by Supra 35-VP, Carl Zeiss where the surface of the samples was treated

with gold deposited in vacuum for 3 min. The optical bandgap E_g was estimated from the UV-2600, SHIMADZU spectrophotometer.

2.5 | Photocatalytic assay

The photocatalytic activity of samples was determined by the discoloration of RhB dye in aqueous solution under UV radiation. RhB dye is widely used as a model dye for the standardization of photocatalytic nanomaterials.[33,34] The dye is a cationic molecule and shows a molecular absorption peak at 554 nm. The pristine PLA and ZN1, ZN3, ZN5, ZN7 and ZN9 samples were cut to 45 x 10 mm and fixed to the inner face of the cuvettes, as shown in the Scheme 2. Each cuvette was filled with a 4 mL aliquot of RhB at 5 ppm. Then, the samples were kept in contact with the dye solution for 60 minutes in the dark to achieve stabilization of adsorption–desorption in the PLA knitted. The cuvettes were kept in a radiation chamber positioned at an angle of 45° at a distance of 13 cm from the lamps and at a temperature never exceeding 30°C. The radiation chamber is made up of two 20 W fluorescent lamps from the Verivide brand and an 18 W ultraviolet black light bulb from Phillips, with emission spectra between 330 and 400 nm. The chamber's radiation system was 13 W m^{-2}, monitored by a radiometer (HD9021, Delta Ohm). The photocatalytic efficiency was monitored by measuring the absorbance at the wavelength of highest intensity of the dye (554 nm) as a function of the irradiation time suffered (t) at 30 min intervals of

collection, using a UV-Shimadzu spectrophotometer 310PC. The reaction kinetics of the discoloration of the RhB solution for each nanocoating sample can be described by Equation (5) fitted to a first order kinetic model:

$$\ln\frac{C0}{C} + k(C0 - C) = krKt \tag{5}$$

where C is the RhB concentration at time t, C_0 is the initial concentration value, and K is the dye adsorption coefficient and k_r is the reaction kinetic constant.

3 | RESULTS AND DISCUSSIONS

3.1 | Morphologic properties of the ZnOQD and ZnOQD coated PLA fabric

The x-ray diffraction pattern of the ZnOQD powder obtained by precipitation synthesis in ethanol is shown in Figure 1. The peaks at positions $2\theta = 31.76°$, $34.40°$ and $36.23°$ are relative to the crystalline planes (100), (002) and (101), respectively, exhibit high intensity while the peaks of less intensity at positions $2\theta = 47.58°$, $56.63°$, $62.88°$ $67.96°$, $72.52°$ and $77.05°$, are related to the crystalline planes (102), (110), (103), (112), (004) and (202), respectively, corresponding to planes of wurtzite structure (JCPDS card: 05-0664), according to the literature.[35,36] The results are presented in the supplementary material (see Table S1) reveal a good agreement with crystallographic database cited, which allows to clarify the formation of ZnO appropriate to the parameters of the unit cells and the reported crystalline structure.

The high intensity and narrow thickness of the peaks, mainly in relation to the planes (100), (002) and (101) in the XRD indicate a polycrystalline structural characteristic of the ZnO nanoparticles powder.[37] From the XRD pattern it is evident the absence of peaks that do not belong to the wurtzite phase, this demonstrates that precipitation synthesis formed ZnO nanoparticles without other structures that differ from the ZnO wurtzite hexagon. Moreover, the excess of ions (OH^-) at pH between 10 and 11 can generate the formation of ZnO in zinc hydroxide however, the hydrogen potential measurement of the ZnOQD colloid resulted in pH 9.4, which corroborates the presence of an only phase on XRD. Although there was no total nucleation of $Zn(OH)_2$ in ZnO nanoparticles, the centrifugation process allowed the residual removal of the $Zn(OH)_2$ growth units formed by the reaction between zinc acetate and potassium hydroxide, similar to what occurs in the mechanism reaction using NaOH as reducing agent.[35]
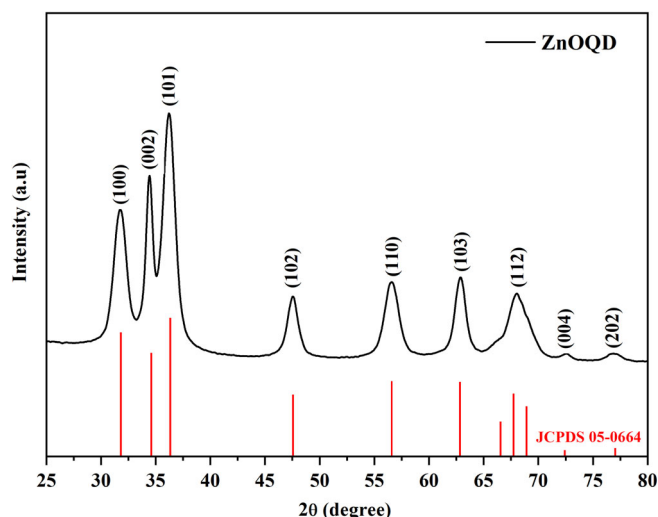

FIGURE 1 X-ray diffraction pattern of ZnOQD [Color figure can be viewed at wileyonlinelibrary.com]

The crystallite size of ZnOQD was determined using debye–scherrer method based at peak of greatest intensity of XRD pattern. As reported, the intensity is a demonstration of preferential crystallographic growth during the formation of nanoparticles.[38] To evaluate the crystallite orientation, a precise analysis of the crystallographic structure was determined through the texture coefficient (TC_{hkl}) based on the intensity values of each plane (hkl) related to the referent peak of greater intensity (101) present in XRD lattice of ZnO and the intensities of the letter JCPDS 05–0664. Thus, TC_{hkl} was calculated following the Equation (6).[39]

$$R_{hkl} = \frac{I_{hkl}}{\sum_{i}^{7} I_{h_i k_i l_i}} \times 100 \tag{6}$$

where R_{hkl} is the relation between the relative intensity I_{hkl} measured from the plane's reflection hkl, in percentage, and $\sum_{i}^{7} I_{h_i k_i l_i}$ is the sum of the reflections intensities at planes (100), (002), (101), (102), (110), (103) and (112) in XRD lattice. The Equation (7) definition to realization of the texture coefficient calculation TC_{hkl} is introduced in the following form:

$$TC_{hkl} = \frac{R_{hkl}}{R_{Shkl}} \tag{7}$$

where R_{hkl} and R_{shkl} are relative intensities corresponding to plans with Müller Indices of ZnO XRD lattice and the JCPDS 05-0664 crystallographic card, respectively. The results of TC_{hkl} is presented in the supplementary material (see Table S2), indicate a preferential orientation to
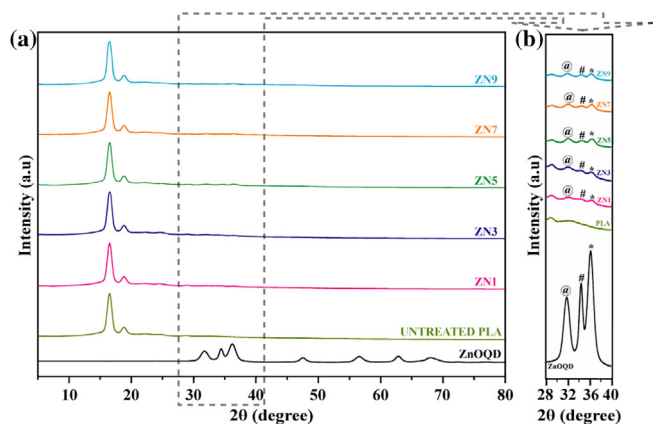
FIGURE 2 XRD pattern of ZnOQD nanocoated PLA and (b) enlargement of the XRD standard of ZN1, ZN3, ZN5, ZN7 e ZN9 between 24° and 40°. PLA, polylactic acid; XRD, X-ray diffraction [Color figure can be viewed at wileyonlinelibrary.com]

the plane (002) with $TC_{200} = 1.32$ since $TC_{hkl} > 1$ indicates a preferred orientation along the plane (hkl) in comparison with the distribution of ZnO nanoparticles.[39] Based on texture coefficient results presented in Table S2 indicate that the nanoparticles have a preferred orientation along the plane (002), then used as a basis for crystallite size using the Equation (8)[40]:

$$D = \frac{k\lambda}{\beta cos\theta} \quad (8)$$

where $k = 0.9$, $\lambda = 0.154$ nm, the x-ray wavelength, β is full width at half maximum and $cos\theta$ is the Bragg's diffraction angle corresponding to the plane (002). The average crystallite size calculated for the ZnO nanoparticles obtained by precipitation was 9.14 nm.

The ZnO nanoparticles coated PLA knitted by LBL assembly was investigated following the XRD patterns as shown in Figure 2a. The presence of two peaks is observed, one of greater intensity at Bragg's diffraction 16.5° corresponding to the plane (110/200) and the other of lesser intensity at Bragg's diffraction 18.8° corresponding to the plane (203), typical of an orthorhombic crystal in the region crystal of the PLA fiber in all analyzed samples.[41,42] This observation demonstrates the morphological properties of the polymer remains unchanged after nanocoating process. Although there is a conformity in the diffraction patterns between untreated PLA knitted fabric and ZnOQD coated PLA they are composed of amorphous polymeric structures interspersed with crystalline polymeric regions, as shown by Bragg's diffraction between 24° and 40° of the XRD in Figure 2b, the samples ZN1, ZN3, ZN5, ZN7 and ZN9 nano-finished show diffraction peaks at Bragg's

diffraction $2\theta = 31.9°$, 34.4° and 36.2° attributed to the (100), (002) and (101) planes, respectively, of the phase ZnOQD wurtzite represented by @, #, and * symbols, respectively.

The chemical compositions on surface of pristine and PDDA functionalized PLA knitted fabric with ZnOQD were analyzed by XPS in order to demonstrate possible surface changes and the types of chemical bonds after the LBL assembly process. Figure 3a,b shows the XPS patterns of pristine of typical C1s and O1s core electron, respectively. The C1s spectra of bare PLA is attributed to three binding energies of 284.9, 286.5 and 288.7 eV to aliphatic carbon bond C—C and/or to the methyl group C—H, C—O bond and ester bond COO— present in the chain polymeric of PLA, respectively.[43] The O1s spectra deconvoluted peaks exhibit two major binding energy peaks at 533.5 eV attributed to oxygen present in ester bonds O—C=O and peak at 531.9 eV attributed to C—OH bond corresponding to oxygen of aliphatic compound.[44] Figure 3c shows the XPS pattern of PDDA functionalized PLA fiber of N1s core level. The N1s spectra, deconvoluted peaks are located at 398.8 and 399.4 eV attributed to nitrogen in the form of amine bonds C—N and N—H, respectively, and peak at 400.37 eV assigned to N^+ species in the PDDA of pyrrolidine ring which corroborates the presence of the polycationic agent on PLA fibers surface, clearly the formation of the LBL nanocoating with the polyelectrolyte due to the existence quaternary ammonium groups in PDDA molecule.[45] Figure 3d shows the XPS patterns of PLA fabric after nine cycles of LBL assembly coating which revels presence of Zn2p peaks in all the samples. The Zn2p spectra deconvoluted exhibit a peak centered on binding energy at 1021.5 eV attributed to Zn 2p3/2 electrons of the ZnO,[46] which confirms the ZnOQD deposition by LBL assembly on PLA fiber. The spectra deconvoluted to O1s corel level (Figure 3e) has a shoulder-shaped peak with a binding energy centered on 531.8 eV corresponding to the Zn—OH bond for oxygen in water molecules present on the ZnO surface.[47] Moreover, the presence of the peak with the highest binding energy at 530 eV corresponding to Zn—O bond can be attributed to the atoms present in the wurtzite polycrystalline structure of ZnO.[48]

The Figure 4a shows TEM image with histogram of nanocrystals size. The micrograph reveals uniform nanoparticles in shape, almost spherical and hexagonal with particle sizes ranging from 4 to 13 nm, however, the histogram shows a distribution of average particle sizes described by a Gaussian function, with a particles size of 8 ± 1.5 nm. In the HRTEM image (Figure 4b), displays a nanoparticle whose spacing of 2.6 Å indicates the orientation of the growth of the ZnO nanocrystals toward the plane (002). Furthermore, it can be seen that the SAED
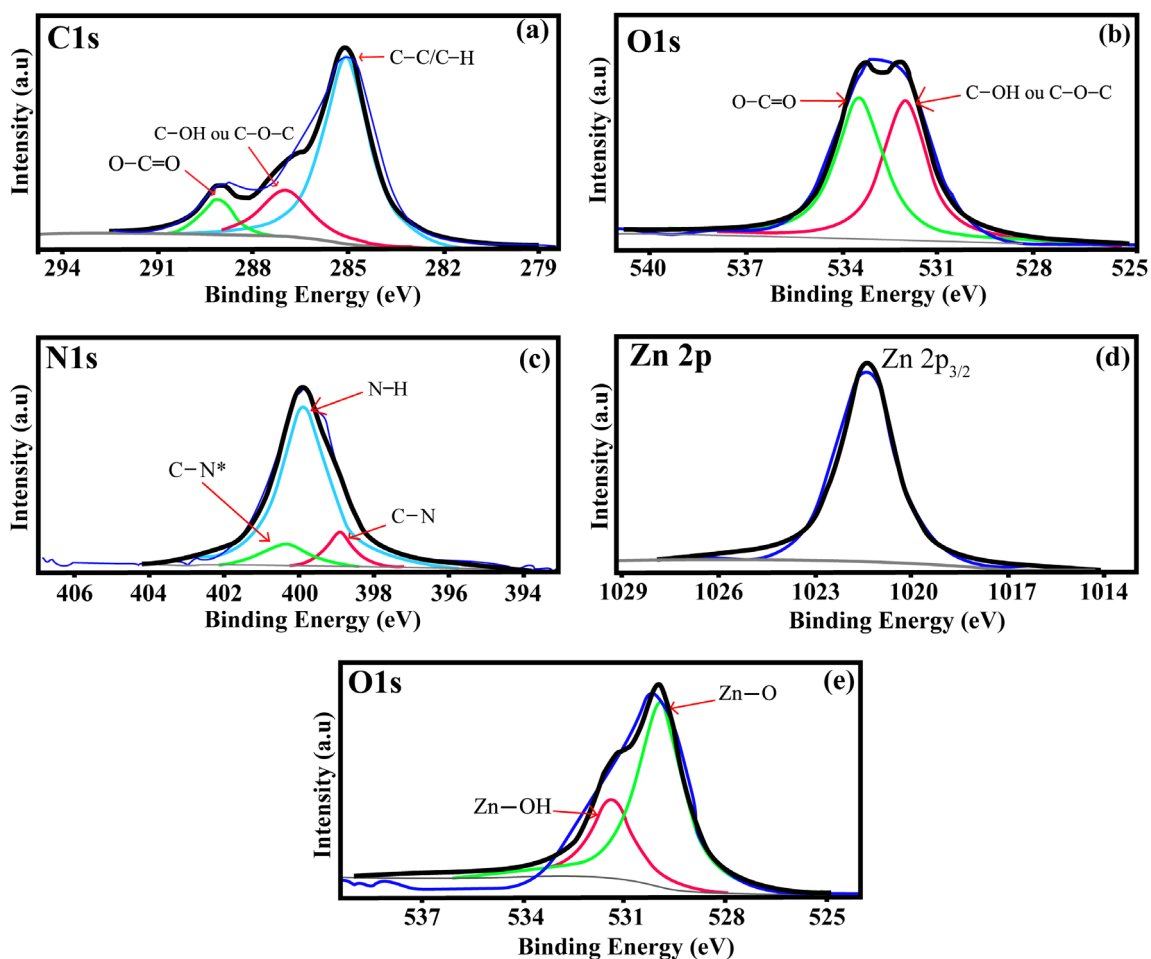
FIGURE 3 C1s and O1s XPS spectra of (a-b) uncoated PLA fabric, N 1s XPS spectra of (c) PLA/PDDA and (d-e) Zn2p and O1s XPS spectra of ZnOQD impregned on PLA fabric samples [Color figure can be viewed at wileyonlinelibrary.com]

FIGURE 4 (a) TEM and particle size distribution, (b) HRTEM and (c) SAED pattern of ZnOQD. HRTEM, high-resolution transmission electron microscopy; SAED, selected area electron diffraction; TEM, transmission electron microscopy [Color figure can be viewed at wileyonlinelibrary.com]
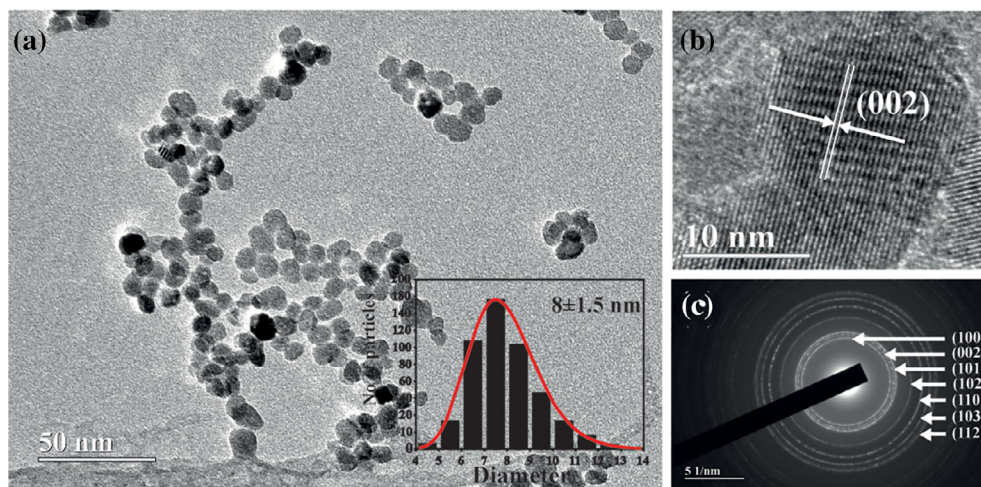
of HRTEM (Figure 4c) shows concentric rings typical of materials of a polycrystalline nature and of high crystallinity[49] corresponding at atomic plans (100), (002), (101), (102), (110) and (103) of ZnO wurtzite phase.[50]

The sample containing pristine (Figure 5a) shows a clean, low-roughness microstructure and smooth in

appearance, typical found in regenerated fiber of this type.[51] FESEM micrographs of PLA fibers coated with 1 cycle (ZN1) (Figure 5b), 3 cycles (ZN3) (Figure 5c), 5 cycles (ZN5) (Figure 5d), 7 cycles (ZN7) (Figure 5e) and 9 cycles (ZN9) (Figure 5f) present layers of PDDA on the longitudinal surface of the fiber after the nanocoating
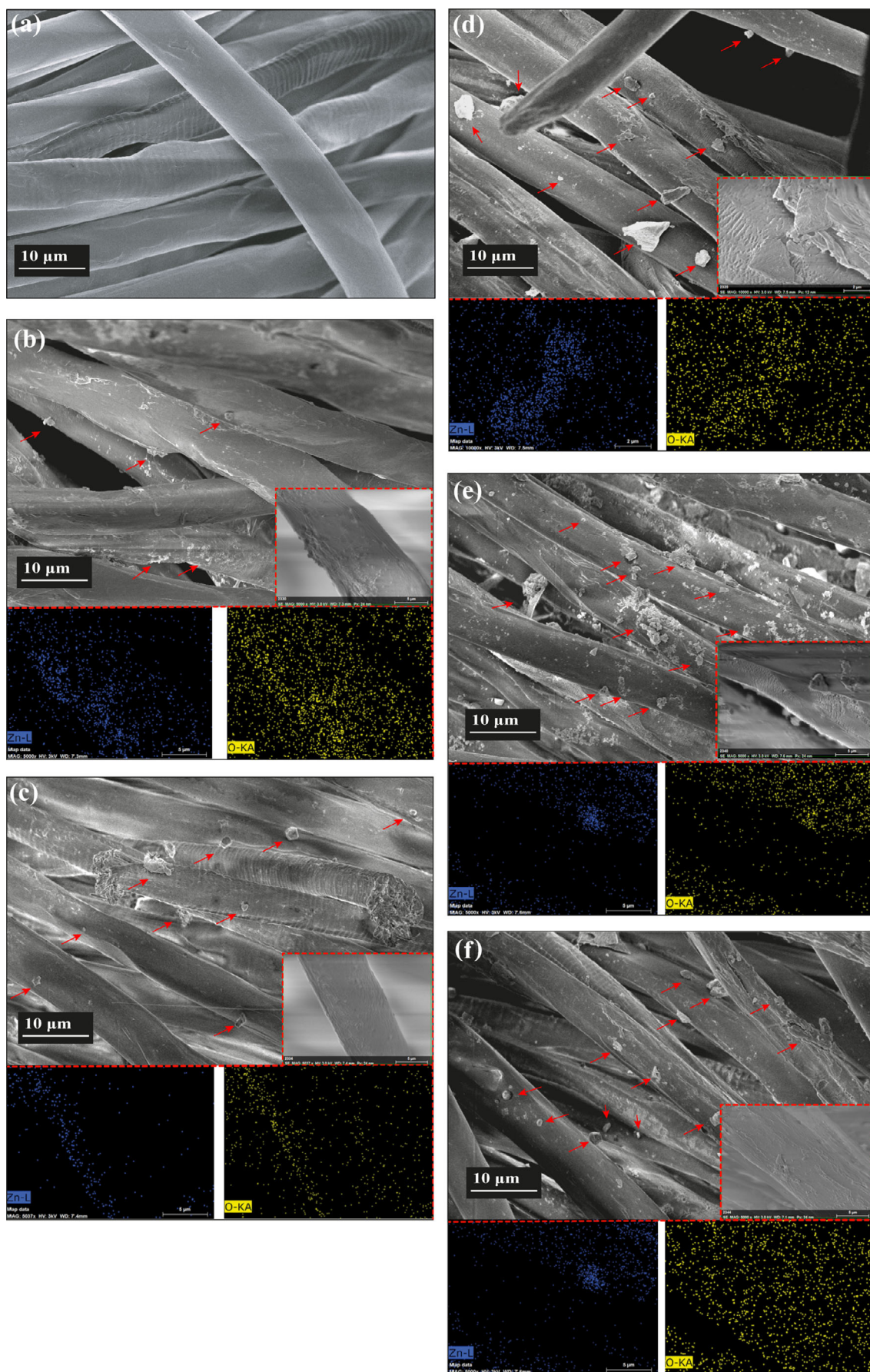
FIGURE 5 FESEM micrographs of the (a) pristine PLA and FESEM micrographs with insights followed by chemical-mapping for the elements Zn and O of (b) ZN1, (c) ZN3, (d) ZN5, (e) ZN7 and (f) ZN9 samples [Color figure can be viewed at wileyonlinelibrary.com]

process, indicated by red arrows. The immobilization process via LBL promoted the deposition of ZnOQD on the PLA fibers, a fact corroborated by the blue identification for the Zn element from superficial elementary mapping and Zn peak in the EDS spectrum (see Figure S1), shows the microstructural superficial change of the PLA fiber present. However, there is also the presence of Cl in the samples, possibly caused by the formation of defect points where there was an increase in the overlap of PDDA layers as the number of LBL cycles increased, therefore, regions of the fiber surface that did not receive the layer. Polycation repel ZnO nanoparticles to migrate to these defect points, forming aggregates.[52] In addition, the formation of hydroxylated metallic species, such as $Zn(OH)_4^{2-}{}_{(aq)}$, $Zn(OH)_4^{2-}{}_{(aq)}$ and $Zn(OH)^{3-}{}_{(aq)}$ ions, generated by the dissociation of ZnO $_{(s)}$ in an aqueous medium containing NaOH increases the amount of dispersed components adsorb more protons on the surface of the metal oxide. Thus, the substrate containing adsorbed PDDA stays in contact with the anionic ZnO solution for a longer time, reducing pH 11 to pH levels close to the isoelectric point of the solution. It was found that ZnO solutions at pH <11 remain unstable, as the accumulation of dissolved cations induces an increase in the average hydrodynamic diameter for the aggregation of ZnO nanoparticles.[53]

Spectroscopy in the UV–vis region of the ZnOQD and PLA knitted fabric with semiconductor were performed to analyze the optical properties before and after the LBL self-assembly coating process. Figure 6a shows the optical gap band (E_g) of the pure ZnO nanocrystal related to its UV–vis absorbance spectrum. It is observed that no other peak besides the ZnO itself present in the UV–vis absorbance spectrum, confirming that we synthesize a pure

metallic oxide. Furthermore, there is a shift in the blue of the strong absorption band in the region at 360 nm corresponding to the effect of quantum confinement, as found in other works.[54]

3.2 | Eg evaluation of ZnOQD and ZnOQD coated PLA knitted fabric

For PLA fibers coated with ZnOQD also show the same deviation from blue, as shown in the diffuse reflectance spectra of Figure 6b, showing that its optical property remained unchanged after the self-assembly process via LBL. The E_g was estimated by extrapolating the linear portion of the absorption curve versus photon energy, applying Wood and Tauc's theory[55] expressed by Equation (9):

$$\alpha h\nu = (h\nu - E_g)^n \tag{9}$$

where α is the absorption coefficient, $h\nu$ is the photon energy and n is the value constant 1/2, adopted for transitions of a direct nature to ZnOQD.[54] For nanocomposites, E_g is derived from the diffuse reflectance spectrum applying the Kubelka–Munk Equation (10) $F(R)$[56]:

$$F(R) = \frac{K}{S} = \frac{(1-R)^2}{2R} \tag{10}$$

where K is the absorption coefficient, S is the scattering coefficient and R is diffuse reflectance. According to Figure 6a, the extrapolation of the curve shows a E_g value of 3.17 eV for ZnOQD, whereas in Figure 6b the E_g values
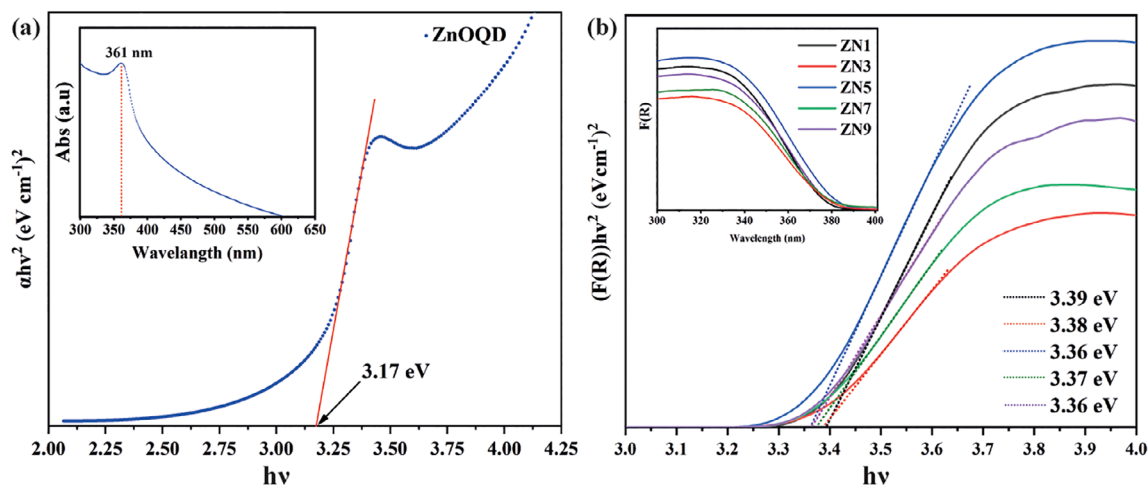

FIGURE 6 Estimated E_g values for (a) ZnOQD and (b) ZN1, ZN3, ZN5, ZN7 and ZN9. The insets show the (a) UV–vis absorbance spectrum of ZnOQD and (b) F(R) of ZN1, ZN3, ZN5, ZN7 and ZN9 [Color figure can be viewed at wileyonlinelibrary.com]

of samples ZN1, ZN3, ZN5, ZN7 and ZN9 were estimated at 3.39, 3.38, 3.36, 3.37 and 3.36 eV, respectively. It is evident that after the immobilization process, the E_g of nanoparticles coated PLA fabric increased in relation to pure ZnOQD. This rise in E_g is a direct response to the contribution of PLA fiber attributed to the insulating properties of aliphatic polymers.[57] Furthermore, it is important to note that pure PLA does not have any optical band.[57] The optical band gap is an intrinsic property of semiconductors, however, a nominal increase in the optical band gap of ZnOQD impregnated fabric was observed, suggesting that as the concentration of ZnO nanoparticles deposited on the substrate increases, greater is the concentration charge carriers of ZnOQD, so this increase in the band gap can be attributed the Bursten–Moss effect.[58] A similar case was reported by Saeed et al., who found an increase in the optical band gap in tin doped indium oxide films deposited on PLA substrate.[59]

3.3 | Photocatalytic evaluation of ZnOQD/PDDA/PLA

The photocatalytic activity of pristine PLA fabric and ZnOQD/PDDA/PLA samples with different assembly cycles of ZnOQD by LBL were estimated based in the initial (Co) and final (C) absorbance ratio at each exposure interval, as shown in Figure 7a. It is observed that the C/Co lines suffered a RhB reduction in the absence of light as a result of the fabric adsorption process, however, the variation of the dye degradation after 360 min of exposure to UV irradiation is greater for the ZnOQD coated PLA fabric more than PLA pristine sample, except for the blank experiment that did not show significant change in concentration at straight line of photolysis sample, as the dye is chemically stable and resistant to UV radiation.[60] The PLA Pristine faded only 25% of RhB dye removed refers to the process of physisorption or physical adsorption between the cationic dye molecule
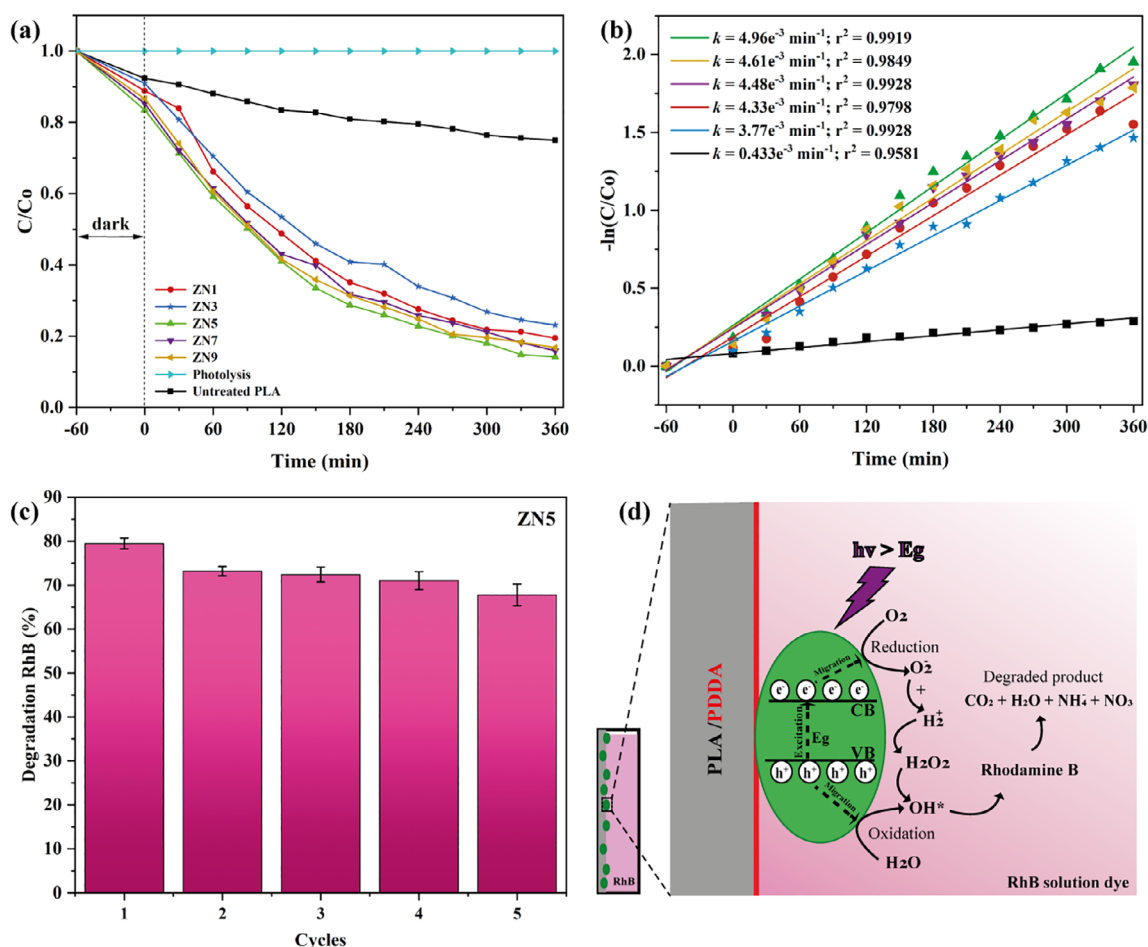

FIGURE 7 (a) C/C$_o$ and (b) −ln(C/C$_0$) variations versus irradiation time of RhB dye of ZnOQD and PLA/PDDA/ZnOQD fabric under UV irradiation, (c) photocatalytic cycles and (d) scheme of the photocatalytic mechanism of PLA/PDDA/ZnOQD fabric [Color figure can be viewed at wileyonlinelibrary.com]
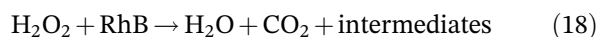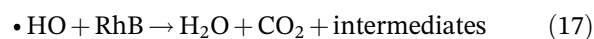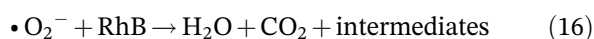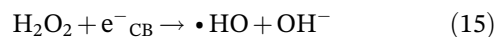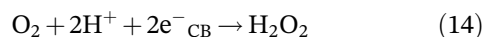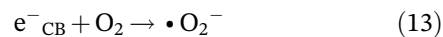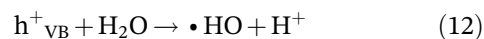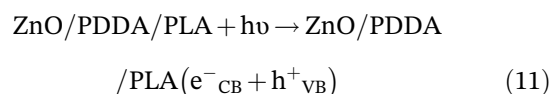
adsorbed on the surface of PLA knitted fabric, which has a slightly anionic and hydrophobic character as it is an aliphatic polyester molecule polymer.[61–63] However, there was greater decolorization of the RhB dye from ZnOQD coated PLA samples, specifically for the Zn5 sample which faded about 85% of the dye after 360 min. This phenomenon is linked to the breaking of Azo bonds of RhB molecule by photogenerated free radicals of ZnOQD during UV irradiation.[64] The reaction kinetics of the discoloration of RhB solution for each coating sample can be described from the slope of the linear graph ln(Co/C) versus time, which displays a straight line confirming the first order degradation kinetic model of Langmuir–Hinshelwood.[65,66] According to Figure 7b shows the estimated values of the kinetic constants and the fit of the quadratic curve (r^2).The degradation efficiency of the dye was 10 times higher for the PLA knitted after coated with ZnOQD than without the nanocoating on PLA pristine, highlighting the greater kinetic constants of the samples ZN5 = $4.96e^{-3}$ min^{-1}, ZN9 = $4.46e^{-3}$ min^{-1} and ZN7 = $4.48e^{-3}$ min^{-1} after 360 min of exposure to UV radiation, with higher values for PLA coated with ZnOQD found for photocatalytic processes in other works.[67,68]

It was found that ZnOQD solutions at pH <11 remain unstable, as the accumulation of dissolved cations induces an increase in the average hydrodynamic diameter for the aggregation of ZnO nanoparticles.[69] A greater amount of nanoparticles allows the formation of active sites to produce reactive oxygen species (ROS) on the surface of the ZnO to react with the dye, obtaining greater photocatalytic activity.[70] However, the results of the photocatalytic efficiency of the nanocomposite revealed that they are independent of the concentration of ZnO on the fiber. As observed in Figure 2s, the ZN9 sample with the most nanoparticle coating cycles degraded 83%, very close to the 80% degraded dye for ZN1 sample. The reason for this result can be interpreted by the lack of homogeneity of the nanocoating greater than 1 LBL cycle, as previously discussed. This allows us to infer that a smaller interaction between nanoparticles and dye, thus a larger particle size increase the charge carrier's recombination rate to produce a smaller amount of reactive oxidative species.[71] Although this limitation is present, it was found that few coating cycles are sufficient to obtain significant results of dye degradation, so it can be carried out at a lower cost for eventual applications. Therefore, the values obtained from hybrid materials based on ZnOQD are a great alternative in advanced oxidative processes in the purification of water with organic contaminants.[72]

Most studies of materials applied in photocatalytic processes are dedicated to samples in the form of powder, especially because nanoparticles have a high reactivity in dye molecules under UV radiation.[72–76] However,

ZnOQD and ZnO nanoparticles can cause significant risks to aquatic and terrestrial species in an eventual industrial use,[77] therefore, it is necessary to retain the nanoparticulate catalyst in the treatment system, which can hamper the process of pollutant degradation in a sustainable manner. Based on this, supports such as functionalized textile fibers with nanoparticles allow not only a great alternative for the retention of these materials, but also allow their use in combined processes of filtration and effluent remediation due to their flexibility properties and good mechanical stability, significant properties for aquatic and terrestrial species in an eventual industrial use.[78] Figure 7c shows the photodegradation efficiency after five cycles of photocatalytic activity of the ZN5 sample. Although there has been a small reduction in this photocatalytic efficiency of the nanocomposite between the RhB degradation process, the ZnOQD nanocomposite has shown to have a good reuse performance.

The photocatalytic degradation mechanism for ZnOQD nanocomposite is shown in Figure 7d. When ZnOQD immobilized on PLA fibers is exposed to UV radiation of energy greater than its band range, electrons from the valence band are excited and transferred to the conduction band (e^-_{CB}), generating the same amount of holes in the valence layer (h^+_{VB}). As a result, excitonic pairs are formed on the catalyst surface where they react with water molecules producing highly ROS that can easily break down the RhB dye into H_2O, CO_2 and other intermediate compounds, as described by Equation (11) to (18).[72,79]

$$ZnO/PDDA/PLA + h\upsilon \rightarrow ZnO/PDDA$$
$$/PLA\left(e^-_{CB} + h^+_{VB}\right) \tag{11}$$

$$h^+_{VB} + H_2O \rightarrow \bullet HO + H^+ \tag{12}$$

$$e^-_{CB} + O_2 \rightarrow \bullet O_2^- \tag{13}$$

$$O_2 + 2H^+ + 2e^-_{CB} \rightarrow H_2O_2 \tag{14}$$

$$H_2O_2 + e^-_{CB} \rightarrow \bullet HO + OH^- \tag{15}$$

$$\bullet O_2^- + RhB \rightarrow H_2O + CO_2 + intermediates \tag{16}$$

$$\bullet HO + RhB \rightarrow H_2O + CO_2 + intermediates \tag{17}$$

$$H_2O_2 + RhB \rightarrow H_2O + CO_2 + intermediates \tag{18}$$

In additional, previous studies using ZnO nanoparticles identified the formation of intermediate compounds such as NO_3 and NH_4^- after photocatalytic processes.[80,81]

This pair can recombine or migrate to the surface of the ZnOQD nanocomposite. If there is migration to the surface, this pair ends up serving as a redox source that reacts with the adsorbed RhB molecule, causing its degradation.

4 | CONCLUSION

ZnOQD with an average diameter of 8 nm were obtained and later coated on PLA knitted fabric. The XPS and XRD analyzes confirmed the presence of ZnOQD on the PLA fiber surface, this fact is corroborated by FESEM micrographs that showed the PLA fibers surface was coated with ZnOQD. Therefore, the LBL self-assembly as a process to functionalization of textiles materials allowed to coated the PLA knitted fabric with ZnOQD and add photocatalytic properties. The samples containing ZnOQD showed photocatalytic activity acting on the photodegradation of RhB under UV irradiation, respecting the rule of a pseudo first order reaction, which showed good application in the treatment of organic contamination as dyes and with the possibility of reusing ZnOQD nanocomposites and more cycles photocatalytic application.

AUTHOR CONTRIBUTIONS
Rivaldo Leonn Bezerra Cabral: Conceptualization (equal); data curation (equal); formal analysis (lead); investigation (equal); methodology (lead); supervision (lead); validation (lead); visualization (lead); writing – original draft (lead); writing – review and editing (lead). **Felipe Mendonça Fontes Galvão:** Data curation (equal); investigation (supporting); validation (supporting); writing – review and editing (supporting). **Kesia Karina Oliveira de Souto Silva:** Data curation (supporting); investigation (supporting); project administration (supporting); visualization (equal); writing – original draft (equal); writing – review and editing (equal). **Brenno Henrique Silva Felipe:** Investigation (supporting); methodology (equal); validation (supporting); visualization (equal); writing – original draft (supporting); writing – review and editing (supporting). **Nivaldo Freire de Andrade Neto:** Data curation (equal); formal analysis (supporting); investigation (supporting); validation (equal); visualization (supporting); writing – review and editing (equal). **Pierre Basílio de Almeida Fechine:** Data curation (equal); formal analysis (supporting); investigation (supporting); resources (equal); supervision (equal); writing – review and editing (equal). **Andrea Zille:** Data curation (equal); formal analysis (equal); supervision (supporting); visualization (supporting); writing – review and editing (supporting). **Suyeon Kim:** Formal analysis (supporting); investigation (supporting); validation (equal); visualization (supporting); writing – review and editing (supporting).

ORCID
Rivaldo Leonn Bezerra Cabral https://orcid.org/0000-0002-9775-5818
Felipe Mendonça Fontes Galvão https://orcid.org/0000-0002-1931-0848
Kesia Karina Oliveira de Souto Silva https://orcid.org/0000-0002-9705-6750
Brenno Henrique Silva Felipe https://orcid.org/0000-0002-7717-0468
Nivaldo Freire de Andrade Neto https://orcid.org/0000-0003-1421-2904
Pierre Basílio de Almeida Fechine https://orcid.org/0000-0002-7822-2354
Andrea Zille https://orcid.org/0000-0001-5299-4164
Suyeon Kim https://orcid.org/0000-0003-1621-1489
José Heriberto Oliveira do Nascimento https://orcid.org/0000-0001-6804-2854

REFERENCES
[1] M. A. Hassaan, A. El Nemr, A. Hassaan, *Am J Environ Sci Eng* **2017**, *1*, 64.
[2] E. Routoula, S. V. Patwardhan, *Environ. Sci. Technol.* **2020**, *54*, 647.
[3] T. Taher, A. Yoshida, A. Lesbani, I. Kurnia, G. Guan, A. Abudula, W. Ueda, *J. Hazard. Mater.* **2021**, *415*, 125635.
[4] H. Mittal, S. M. Alhassan, S. S. Ray, *J. Environ. Chem. Eng.* **2018**, *6*, 7119.
[5] Q. Feng, B. Gao, Q. Yue, K. Guo, *Chemosphere* **2021**, *262*, 128416.
[6] A. Raj, A. Yadav, A. P. Rawat, A. K. Singh, S. Kumar, A. K. Pandey, R. Sirohi, A. Pandey, *Environ. Technol. Innov.* **2021**, *23*, 101556.

[7] H. Anwer, A. Mahmood, J. Lee, K.-H. Kim, J.-W. Park, A. C. K. Yip, *Nano Res.* **2019**, *12*, 955.

[8] A. Mills, R. H. Davies, D. Worsley, *Chem. Soc. Rev.* **1993**, *22*, 417.

[9] K. Maeda, *J. Photochem. Photobiol. C* **2011**, *12*, 237.

[10] P. Nandi, D. Das, *Appl. Surf. Sci.* **2019**, *465*, 546.

[11] T. Ahmed, T. Edvinsson, *J. Phys. Chem. C* **2020**, *124*, 6395.

[12] W. A. A. Mohamed, H. H. Abd El-Gawad, S. D. Mekkey, H. R. Galal, A. A. Labib, *Opt. Mater.* **2021**, *118*, 111242.

[13] W. A. A. Mohamed, H. T. Handal, I. A. Ibrahem, H. R. Galal, H. A. Mousa, A. A. Labib, *J. Hazard. Mater.* **2021**, *404*, 123962.

[14] W. A. A. Mohamed, I. A. Ibrahem, A. M. El-Sayed, H. R. Galal, H. Handal, H. A. Mousa, A. A. Labib, *Adv. Powder Technol.* **2020**, *31*, 2555.

[15] W. A. A. Mohamed, H. H. Abd El-Gawad, S. D. Mekkey, H. R. Galal, A. A. Labib, *Arab. J. Chem.* **2022**, *15*, 103593.

[16] R. Khan, M. S. Hassan, L.-W. Jang, J. H. Yun, H.-K. Ahn, M.-S. Khil, I.-H. Lee, *Ceram. Int.* **2014**, *40*, 14827.

[17] X. Chen, Z. Wu, D. Liu, Z. Gao, *Nanoscale Res. Lett.* **2017**, *12*, 1.

[18] Z. L. Wang, X. Y. Kong, Y. Ding, P. Gao, W. L. Hughes, R. Yang, Y. Zhang, *Adv. Funct. Mater.* **2004**, *14*, 943.

[19] H. Kumar, Y. Kumar, K. Singh, S. Kumar, G. Rawat, C. Kumar, B. N. Pal, S. Jit, *Electron. Lett.* **2017**, *53*, 262.

[20] M. Pabbi, S. K. Mittal, *Anal. Methods* **2017**, *9*, 1672.

[21] Q. Qiao, B. H. Li, C. X. Shan, J. S. Liu, J. Yu, X. H. Xie, Z. Z. Zhang, T. B. Ji, Y. Jia, D. Z. Shen, *Mater. Lett.* **2012**, *74*, 104.

[22] T. Jin, D. Sun, J. Y. Su, H. Zhang, H. J. Sue, *J. Food Sci.* **2009**, *74*, M46.

[23] J. M. Luther, J. Gao, M. T. Lloyd, O. E. Semonin, M. C. Beard, A. J. Nozik, *Adv. Mater.* **2010**, *22*, 3704.

[24] L. Irimpan, V. P. N. Nampoori, P. Radhakrishnan, *J. Appl. Phys.* **2007**, *102*, 063524.

[25] D. Bera, L. Qian, T. K. Tseng, P. H. Holloway, *Dent. Mater.* **2010**, *3*, 2260.

[26] R. Li, J. Che, H. Zhang, J. He, A. Bahi, F. Ko, *J. Nanopart. Res.* **2014**, *16*, 1.

[27] S. Schmitt-Rink, D. S. Chemla, D. A. B. Miller, *Adv. Phys.* **1989**, *38*, 89.

[28] J. Wang, T. Tsuzuki, L. Sun, X. Wang, *J. Am. Ceram. Soc.* **2009**, *92*, 2083.

[29] I. Bhatt, B. N. Tripathi, *Chemosphere* **2011**, *82*, 308.

[30] Q. Tang, L. Lin, X. Zhao, K. Huang, J. Wu, *Langmuir* **2012**, *28*, 3972.

[31] C. Pacholski, A. Kornowski, H. Weller, *Angew. Chem. Int. Ed.* **2002**, *41*, 1188.

[32] T. V. Kolekar, H. M. Yadav, S. S. Bandgar, P. Y. Deshmukh, *Indian Streams Res J* **2011**, *1*, 1.

[33] X. Zhang, C. Shao, Z. Zhang, J. Li, P. Zhang, M. Zhang, J. Mu, Z. Guo, P. Liang, Y. Liu, *ACS Appl. Mater. Interfaces* **2012**, *4*, 785.

[34] W. Yang, B. Zhang, N. Ding, W. Ding, L. Wang, M. Yu, Q. Zhang, *Ultrason. Sonochem.* **2016**, *30*, 103.

[35] S. S. Alias, A. B. Ismail, A. A. Mohamad, *J. Alloys Compd.* **2010**, *499*, 231.

[36] M. Ahmad, Z. Hong, E. Ahmed, N. R. Khalid, A. Elhissi, W. Ahmad, *Ceram. Int.* **2013**, *39*, 3007.

[37] K. Gautam, I. Singh, P. K. Bhatnagar, K. R. Peta, *Superlattice. Microst.* **2016**, *93*, 101.

[38] R. Dom, H. G. Kim, P. H. Borse, *CrystEngComm* **2014**, *16*, 2432.

[39] L. P. Berube, G. L'Espérance, *J. Electrochem. Soc.* **1989**, *136*, 2314.

[40] M. Saleem, L. Fang, H. B. Ruan, F. Wu, Q. L. Huang, C. L. Xu, C. Y. Kong, *Int J Phys Sci* **2012**, *7*, 2971.

[41] M. B. Bilal, P. Viallier-Raynard, B. Haidar, G. Colombe, A. Lallam, *Text. Res. J.* **2011**, *81*, 838.

[42] N. Reddy, D. Nama, Y. Yang, *Polym. Degrad. Stab.* **2008**, *93*, 233.

[43] R. A. Quirk, M. C. Davies, S. J. B. Tendler, W. C. Chan, K. M. Shakesheff, *Langmuir* **2001**, *17*, 2817.

[44] S. Amor, M. Jacquet, P. Fioux, M. Nardin, *Appl. Surf. Sci.* **2009**, *255*, 5052.

[45] Y. Ogawa, Y. Arikawa, T. Kida, M. Akashi, Y. Ogawa, A. Yuya, K. Toshiyuki & A. Mitsuru, *Langmuir* **2008**, *24*, 8606.

[46] J. Chastain, R. C. King Jr., Perkin-Elmer Corporation **1992**, *40*, 221.

[47] M. Wang, F. Ren, J. Zhou, G. Cai, L. Cai, Y. Hu, D. Wang, Y. Liu, L. Guo, S. Shen, *Sci. Rep.* **2015**, *5*, 1.

[48] M. Gong, Q. Liu, B. Cook, B. Kattel, T. Wang, W.-L. Chan, D. Ewing, M. Casper, A. Stramel, J. Z. Wu, *ACS Nano* **2017**, *11*, 4114.

[49] V. Singh, P. K. Sharma, P. Chauhan, *Mater. Charact.* **2011**, *62*, 43.

[50] R.-O. Moussodia, L. Balan, C. Merlin, C. Mustin, R. Schneider, *J. Mater. Chem.* **2010**, *20*, 1147.

[51] A. Mujica-Garcia, S. Hooshmand, M. Skrifvars, J. M. Kenny, K. Oksman, L. Peponi, *RSC Adv.* **2016**, *6*, 9221.

[52] K. W. Seong, Y. S. Ryu, I. Kim, S. H. Kim, *J. Appl. Polym. Sci.* **2019**, *136*, 47760.

[53] M. O. Fatehah, H. A. Aziz, S. Stoll, *J. Colloid Sci. Biotechnol.* **2014**, *3*, 75.

[54] X. Liu, X. Xing, Y. Li, N. Chen, I. Djerdj, Y. Wang, *New J. Chem.* **2015**, *39*, 2881.

[55] D. L. Wood, J. Tauc, *Phys L Rev B* **1972**, *5*, 3144.

[56] L. Tolvaj, K. Mitsui, D. Varga, *Wood Sci. Technol.* **2011**, *45*, 135.

[57] K. K. Gupta, P. K. Mishra, P. Srivastava, M. Gangwar, G. Nath, P. Maiti, *Appl. Surf. Sci.* **2013**, *264*, 375.

[58] A. K. Anbalagan, S. Gupta, A. Kumar, S.-C. Haw, S. S. Kulkarni, N.-H. Tai, F.-G. Tseng, K. C. Hwang, C.-H. Lee, *ACS Omega* **2020**, *5*, 15129.

[59] U. Saeed, M. S. Abdel-Wahab, V. K. Sajith, M. S. Ansari, A. M. Ali, H. A. Al-Turaif, *Bull. Mater. Sci.* **2019**, *42*, 1.

[60] Q. Wang, G. Yun, Y. Bai, N. An, J. Lian, H. Huang, B. Su, *Appl. Surf. Sci.* **2014**, *313*, 537.

[61] N. Mohammad, Y. Atassi, *Sci. Rep.* **2020**, *10*, 1.

[62] C. S. Ho, N. H. Z. Abidin, M. W. Nugraha, N. S. Sambudi, F. Ali, M. D. H. Wirzal, L. D. Kasmiarno, S. A. Adli, *Fibers Polymers* **2020**, *21*, 1212.

[63] C.-C. Wang, L.-H. Lin, C.-W. Chen, Y.-C. Lo, *Polymer* **2017**, *9*, 371.

[64] N. Tripathy, R. Ahmad, H. Kuk, Y.-B. Hahn, G. Khang, *Ceram. Int.* **2016**, *42*, 9519.

[65] K. V. Kumar, K. Porkodi, F. Rocha, *Catal. Commun.* **2008**, *9*, 82.

[66] F. Di Fonzo, C. S. Casari, V. Russo, M. F. Brunella, A. Li Bassi, C. Bottani, *Nanotechnology* **2009**, *20*, 015604.

[67] K. Vidhya, M. Saravanan, G. Bhoopathi, V. P. Devarajan, S. Subanya, _Appl. Nanosci._ **2015**, _5_, 235.

[68] H. J. Lee, Y. Jin, S. S. Park, S. S. Hong, G. D. Lee, _Appl Chem Eng_ **2015**, _26_, 356.

[69] D. Yu, R. Cai, Z. Liu, _Spectrochim. Acta, Part A_ **2004**, _60_, 1617.

[70] M. I. H. Chowdhury, M. S. Hossain, M. A. S. Azad, M. Z. Islam, M. A. Dewan, _Int. J. Sci. Eng. Res._ **2018**, _9_, 1646.

[71] D. Jassby, J. Farner Budarz, M. Wiesner, _Environ. Sci. Technol._ **2012**, _46_, 6934.

[72] C. B. Ong, L. Y. Ng, A. W. Mohammad, _Renew. Sust. Energ. Rev._ **2018**, _81_, 536.

[73] O. Mekasuwandumrong, P. Pawinrat, P. Praserthdam, J. Panpranot, _Chem. Eng. J._ **2010**, _164_, 77.

[74] M. A. Ahmed, E. E. El-Katori, Z. H. Gharni, _J. Alloys Compd._ **2013**, _553_, 19.

[75] H. N. Tien, V. H. Luan, L. T. Hoa, N. T. Khoa, S. H. Hahn, J. S. Chung, E. W. Shin, S. H. Hur, _Chem. Eng. J._ **2013**, _229_, 126.

[76] T. R. Giraldi, G. V. F. Santos, V. R. Mendonça, C. Ribeiro, I. T. Weber, _J. Nanosci. Nanotechnol._ **2011**, _11_, 3635.

[77] H. Ma, P. L. Williams, S. A. Diamond, _Environ. Pollut._ **2013**, _172_, 76.

[78] H. Böttcher, B. Mahltig, J. Sarsour, T. Stegmaier, _J. Sol-Gel Sci. Technol._ **2010**, _55_, 177.

[79] J. Duraimurugan, S. Shanavas, R. Ramesh, R. Acevedo, P. M. Anbarasan, P. Maadeswaran, _Optik_ **2020**, _202_, 163607.

[80] Y. Zhang, J. Zhou, Z. Li, Q. Feng, _J. Mater. Sci._ **2018**, _53_, 3149.

[81] Z. Zhu, Y. Chen, Y. Gu, F. Wu, W. Lu, T. Xu, W. Chen, _Water Res._ **2016**, _93_, 296.

SUPPORTING INFORMATION

Additional supporting information may be found in the online version of the article at the publisher's website.

How to cite this article: R. L. B. Cabral, F. M. F. Galvão, K. K. O. de Souto Silva, B. H. S. Felipe, N. F. de Andrade Neto, P. B. de Almeida Fechine, A. Zille, S. Kim, J. H. O. do Nascimento, _J. Appl. Polym. Sci._ **2022**, e52381. https://doi.org/10.1002/app.52381